Prediction of unsteady heat transfer from a cylinder in crossflow

By S. T. Bose, B. C. Wang† AND M. Saeedi†

The accuracy of a tensorial eddy diffusivity subgrid scale model for large-eddy simulation (LES) of passive scalar transport is investigated for a heated cylinder in crossflow at $Re = 3000$ and 8900. LES at the higher Reynolds number relies on local mesh refinement in the near wake of the cylinder using an estimate of subgrid scale (SGS) fluctuations of the passive scalar field. Predictions of mean and fluctuating heat transfer at both Reynolds numbers agree reasonably well with the experimental measurements of Nakamura & Igarashi (2004).

1. Introduction

The dynamics of a passive scalar transported by a background turbulent flow are often used to describe the dispersion of pollutants or the temperature of a fluid when the variation in the density is small. The prediction of heat transfer, in particular, is often of paramount importance for engineering systems. For instance, the structural integrity of turbine blades downstream of the combustor in a gas turbine engine is dependent on the amount of heat transferred to the surface from the incident hot gases (an extensive discussion of passive scalar transport in turbulent flows can be found in Warhaft 2000). Large-eddy simulation (LES) has been a popular choice for studying passive scalar transport where the large eddies primarily responsible for the mixing of the scalar are directly solved. However, the modeling of subgrid scale (SGS) scalar fluxes (or heat fluxes) for LES has not received as much attention as the closure models for the filtered momentum equation. Many recent studies that have investigated the accuracy of scalar SGS models have focused on traditional wall-bounded shear flows (Denev *et al.* 2008; Li *et al.* 2011; Inagaki *et al.* 2012), while the present study investigates SGS scalar flux models in separated flows.

The objective of this validation study is to predict the heat transfer from a circular cylinder in crossflow using a tensorial eddy diffusivity SGS model for the passive scalar (temperature) flux. The accuracy of the SGS model at coarse resolutions and higher Reynolds numbers in a separated flow will be assessed. A brief description of the SGS model investigated, the setup of the cylinder in crossflow, and the SGS fluctuation based mesh refinement criteria are given in Section 2. Results and comparison to the experimental measurements are discussed in Section 3, and some directions for continuing work are offered in Section 4.

† Department of Mechanical Engineering, University of Manitoba, Canada

2. SGS modeling for LES of passive scalar transport

2.1. *Dynamic tensorial eddy-diffusivity SGS model*

The filtered equations for the transport of a passive scalar field by an incompressible fluid are given by

$$\frac{\partial \bar{T}}{\partial t} + \frac{\partial \bar{u}_j \bar{T}}{\partial x_j} = \alpha \frac{\partial^2 \bar{T}}{\partial x_j \partial x_j} - \frac{\partial q_j}{\partial x_j}, \tag{2.1}$$

$$q_j = \overline{u_j T} - \bar{u}_j \bar{T}, \tag{2.2}$$

where $\bar{T}$ and $\bar{u}_j$ are the filtered scalar (temperature) and filtered velocity fields, respectively and α denotes the scalar (thermal) diffusion coefficient. This temperature equation in Eq. (2.1) is solved in addition to the filtered momentum equations governing the evolution of the velocity field, $\bar{u}_j$. The tensorial eddy diffusivity model based on a generalized gradient-diffusion hypothesis of Wang *et al.* (2007, 2008) is used to model the unclosed SGS heat flux, q_j defined in Eq. (2.2),

$$q_j = -C_P \bar{\Delta}^2 |\bar{S}| \frac{\partial \bar{T}}{\partial x_j} - C_G \bar{\Delta}^2 \bar{S}_{jk} \frac{\partial \bar{T}}{\partial x_k}, \tag{2.3}$$

where the coefficients, $C_P\bar{\Delta}^2$ and $C_G\bar{\Delta}^2$, are computed dynamically. This model will henceforth be referred to as the dynamic linear tensor diffusivity model (DLTD). Constructing the appropriate Germano identity for the SGS heat flux and performing a least squares minimization (Moin *et al.* 1991; Lilly 1992) yields the following 2×2 system for the coefficients:

$$\begin{bmatrix} P_j P_j & G_j P_j \\ G_j P_j & G_j G_j \end{bmatrix} \begin{bmatrix} C_P \bar{\Delta}^2 \\ C_G \bar{\Delta}^2 \end{bmatrix} = - \begin{bmatrix} L_j P_j \\ L_j G_j \end{bmatrix}. \tag{2.4}$$

Given a test filter, $\hat{G}$, and the ratio of the length scales of the test filter and grid scale, Δ_R, the quantities L_j, P_j, and G_j are defined as

$$L_j = \widehat{\bar{u}_j \bar{T}} - \hat{\bar{u}}_j \hat{\bar{T}}, \tag{2.5}$$

$$P_j = \Delta_R^2 |\hat{\bar{S}}| \frac{\partial \hat{\bar{T}}}{\partial x_j} - \widehat{|\bar{S}| \frac{\partial \bar{T}}{\partial x_j}}, \tag{2.6}$$

$$G_j = \Delta_R^2 \hat{\bar{S}}_{jk} \frac{\partial \hat{\bar{T}}}{\partial x_k} - \widehat{\bar{S}_{jk} \frac{\partial \bar{T}}{\partial x_k}}. \tag{2.7}$$

For the current study, the quantities that appear on the right hand side and in the coefficient matrix of Eq. (2.4) are locally averaged to alleviate large oscillations in the C_P and C_G fields. In addition, negative values of C_P are clipped in order to avoid instabilities associated with negative diffusion coefficients. The dynamic Vreman model (DVM) is used to close the subgrid stresses in the momentum equations for all of the following simulations unless otherwise noted (Lee *et al.* 2010; Vreman 2004).

2.2. *Validation case: heat transfer to a cylinder in crossflow*

The validation case under investigation is the heat transfer from a heated circular cylinder in crossflow experimentally measured by Nakamura & Igarashi (2004). Because the

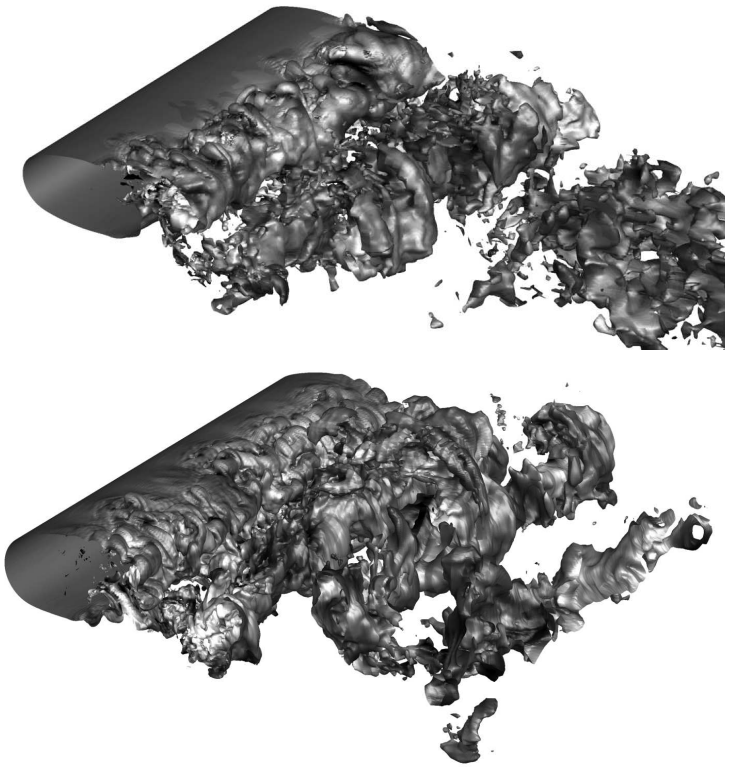

FIGURE 1. Isosurface of normalized temperature, $\hat{T} = 0.04$, colored by spanwise velocity in the near wake of the cylinder at $Re = 3000$ (top) and $Re = 8900$ (bottom). Grayscale contours are from $-0.25U_\infty$ (black) to $0.25U_\infty$ (white).

overheat ratio of the cylinder to the ambient air is small, we solve the incompressible flow equations and treat the temperature as a passive scalar. The cylinder surface is isothermal with a unitary normalized temperature, $\hat{T} = (T - T_\infty) / (T_{cyl} - T_\infty) = 1$. The incident flow has a uniform temperature, T_∞ ($\hat{T} = 0$), and a Prandtl number, Pr, equal to 0.7. The flow is computed using a second-order, unstructured finite volume solver, *cliff*, provided from Cascade Technologies. The surface of the cylinder is parameterized by an azimuthal angle, ϕ, which is equal to 0° at the front stagnation point, 90° close to the separation of the laminar boundary layer and 180° at the rear stagnation location. Figure 1 shows an isosurface of the normalized temperature, $\hat{T} = 0.04$, colored by the spanwise velocity at the two Reynolds numbers studied, $Re = 3000$ and 8900. Both Reynolds numbers investigated are subcritical as can be seen by the laminar separated shear layer that breaks down into turbulence downstream of the cylinder. The laminar shear layer transitions closer to the cylinder and the turbulent fluctuations are also visually stronger at the higher Reynolds number.

The heat transfer on the rear side of the cylinder has been shown to be a strong function of Reynolds number in many experimental studies (Nakamura & Igarashi 2004; Scholten & Murray 1998) and thus will exhibit some sensitivity to the choice of the SGS models used for the momentum and temperature equations. Additionally, prediction of the heat transfer in the wake of the cylinder has very different requirements than the

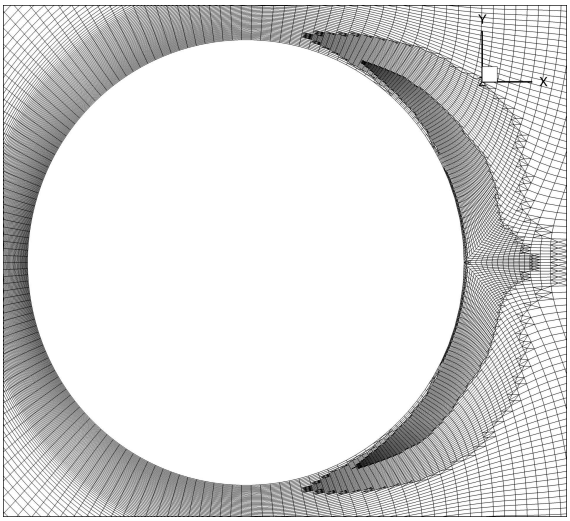

FIGURE 2. Locally refined mesh in the near wake of the cylinder for $Re = 8900$ adapted using $\hat{T}^{*2}$ criterion.

heat transfer characteristics of wall-bounded shear flows (which are closely linked to the resolution of near-wall turbulent structures).

2.3. *Scalar SGS fluctuation based mesh adaptation*

The scalar SGS model in Eq. (2.3) will fail to predict the surface heat transfer coefficients at a coarse resolution, as will be demonstrated in the following section. The standard LES methodology to remedy the poor agreement between numerical and experimental results is to perform a nearly global mesh refinement in order to capture a wider range of scales. This brute force refinement procedure is inefficient and untenable at increasingly large Reynolds numbers. The current study leverages the use of an unstructured mesh and utilizes the local, anisotropic mesh refinement tool, *adapt* (modified from a version provided by Cascade Technologies). Because the surface heat transfer is the quantity of interest, the mesh is refined based on an estimate of the SGS temperature fluctuation energy from the solution of a coarse LES. The SGS temperature fluctuation energy is estimated by

$$\hat{T}^{*2}(x) = \left(\bar{T} - \bar{\bar{T}}\right)^2, \tag{2.8}$$

and the mesh is refined isotropically if $\hat{T}^{*2}$ on the coarse mesh exceeds a given threshold. This strategy is similar to the one employed by Bose *et al.* (2011) where the mesh refinement was dictated by an estimate of the SGS kinetic energy. Additionally, it can be shown that the T^{*2} criterion is bounded from above by the exact $\overline{T'T'}$ for positive filters. Figure 2 shows a slice of the adapted mesh in the near wake of the cylinder for the $Re = 8900$ case. From a single coarse mesh calculation, the adaptation procedure is repeated three times with increasing thresholds. The first two adaptation iterations refine the grid throughout the near wake downstream of where the separated shear layer transitions. The last adaptation iteration creates a very fine mesh close to the surface of the cylinder near the rear stagnation point.

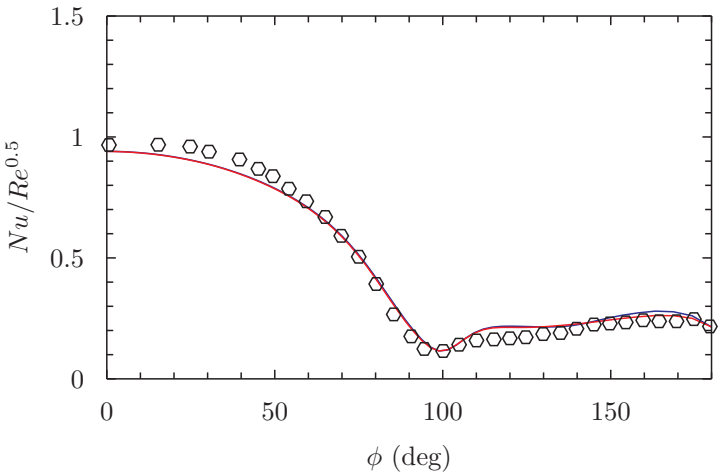

FIGURE 3. Normalized mean Nusselt number on the cylinder surface at $Re = 3000$ (7M cvs); —— DVM/DLTD, —— no-model, ∘ experiment (Nakamura & Igarashi 2004).

3. Results and discussion

3.1. $Re = 3000$

Figures 3 and 4 show the mean and fluctuating Nusselt number predictions on the surface of the cylinder in crossflow at $Re = 3000$. Both the no-model and dynamic SGS modeled LES show similar results, which are in good agreement with the experimentally measured values. On the rear side of the cylinder, the use of the dynamic SGS model corrects a slight overprediction of the no-model case in the root mean squared (rms) fluctuations of the Nusselt number, but the predictions are nearly identical otherwise. There are discrepancies between the LES and experiment on the front side of the cylinder corresponding to the region where the boundary layer is laminar. The experimentally reported mean Nusselt numbers in the laminar boundary layer are elevated when compared to other experiments of heated subcritical cylinders in crossflow (Schmidt & Wenner 1941). The underprediction of the Nusselt number fluctuations however is not explained by comparing different experiments. However, there are small amounts of freestream turbulence present in the experiments that are not matched by the quiescent inflow of the LES which may explain the remaining differences.

3.2. $Re = 8900$

An LES of the cylinder in crossflow using the dynamic SGS models was performed at $Re = 8900$ using the same resolution as the LES in the preceding section at $Re = 3000$ (subsequently referred to as the coarse LES). The predictions of the mean and fluctuating Nusselt numbers compared against the experimental measurements are shown in Figures 5 and 6. The coarse LES severely underestimates both the mean and rms fluctuations on the rear side of the cylinder, especially for $\phi > 120°$. This underprediction could be related to either insufficient resolution of the near-wake turbulent fluctuations or insufficient resolution of the aft thermal boundary layer. There is also a slight overprediction of the rms fluctuations of the Nusselt numbers at the front stagnation point which is persistent even with additional statistical sampling. The mesh is then adapted using the procedure that is described in Section 2.3. The nested grid refinement in the near-wake of the cylinder added roughly an additional 3M cells, and an additional LES was performed

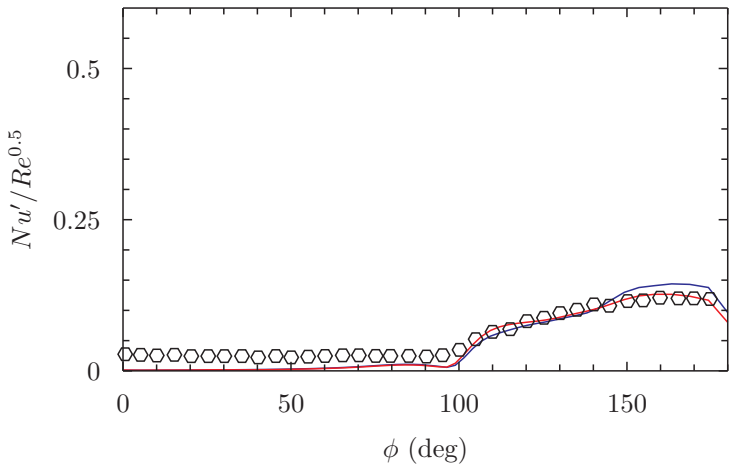

FIGURE 4. Normalized rms Nusselt number fluctuations on the cylinder surface at $Re = 3000$ (7M cvs); —— DVM/DLTD, —— no-model, ∘ experiment (Nakamura & Igarashi 2004).

on this refined mesh using the dynamic SGS models (subsequently referred to as the fine LES). Note that the resolution of the "fine LES" remains much coarser than those used in other DNS and LES studies of a cylinder in crossflow at a nearby Reynolds number, $Re = 10^4$ (Dong *et al.* 2006; Khalighi *et al.* 2010). However, the predictions of the mean and fluctuating Nusselt numbers on the finer mesh are in close agreement with the experimental measurements as seen in Figures 5 and 6. The decrease in the Nusselt number fluctuations near $\phi = 90°$ is slightly delayed in both simulations compared to the experiment, suggesting that the boundary layer separation occurs at slightly different locations. There is also an underprediction of the mean and rms Nusselt numbers very close to the rear stagnation point for $\phi > 175°$.

Figure 7 shows a partial time history of the Nusselt numbers recorded at two different azimuthal locations of the fine LES. The mean Nusselt number is increasingly biased by very strong, intermittent events as the rear stagnation point is approached as reported by Nakamura & Igarashi (2004). While these strong intermittent events are present at $\phi = 150°$ (and other smaller angles), there is little evidence of these events at $\phi = 180°$. Figure 8 shows the power spectral density (PSD) of the Nusselt number fluctuations at three different locations on the rear-side of the cylinder ($\phi = 130°, 150°, 180°$). The frequencies in Figure 8 are normalized by the Strouhal number associated with the vortex shedding, $St_0 = 0.202 \pm 0.01$. It has been previously observed that there was a peak at the shedding frequency at $\phi = 150°$ that appears for $Re > 7000$, which is confirmed in the spectra shown. This shedding frequency peak is absent at the other azimuthal angles in both the experiment and in the current computation. This suggests that while the qualitative behavior of the near-wake region is captured, the model fails to provide the necessary flux to capture either the mean or rms fluctuating Nusselt number near the rear stagnation point. It is possible that poor mesh quality at the rear stagnation point also suppresses the heat transfer from the cylinder. Additionally, given the long residence time of structures inside the recirculation region in the wake of the cylinder, it is possible that the statistical sampling time is insufficient to describe the heat transfer very close to the rear stagnation point.

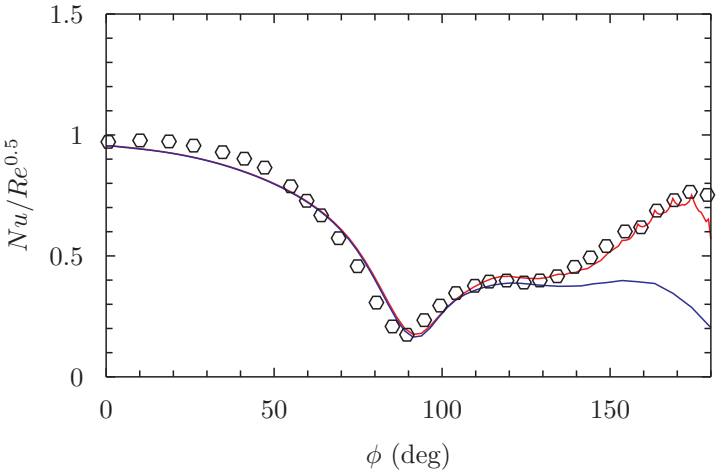

FIGURE 5. Normalized mean Nusselt number on the cylinder surface at $Re = 8900$; —— coarse LES (7M cvs, DVM/DLTD), —— fine LES (10M cvs, DVM/DLTD, adapted mesh), ∘ experiment (Nakamura & Igarashi 2004).

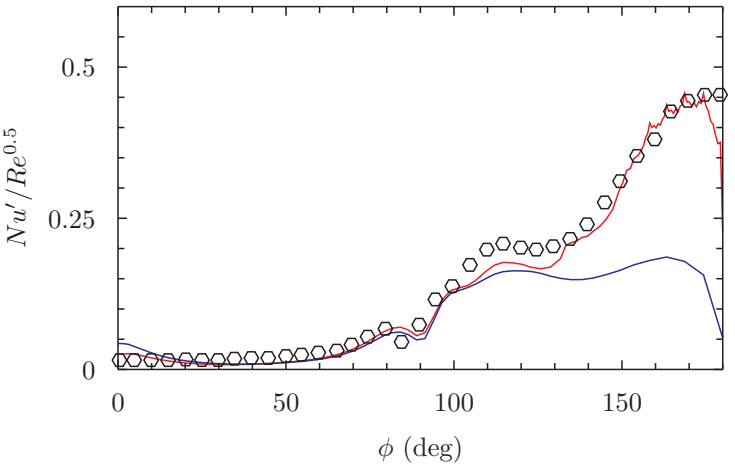

FIGURE 6. Normalized rms Nusselt number fluctuations on the cylinder surface at $Re = 8900$; —— coarse LES (7M cvs, DVM/DLTD), —— fine LES (10M cvs, DVM/DLTD, adapted mesh), ∘ experiment (Nakamura & Igarashi 2004).

4. Concluding remarks & future work

Large eddy simulations of a heated cylinder in crossflow at $Re = 3000$ and 8900 are performed. Predictions of the mean and fluctuating heat transfer from the cylinder are in satisfactory agreement with the experimental measurements of Nakamura & Igarashi (2004). A local mesh adaptation strategy based on the estimated SGS temperature fluctuations was successful in correcting an underprediction of the Nusselt number on the rear side of the cylinder predicted by coarser simulations. However, due to the lack of available validation data, the accuracy of the SGS models can only be indirectly assessed through their effect on the heat transfer predicted at the cylinder surface. The contributions from the SGS models are largest in the wake of the cylinder away from the boundary, and

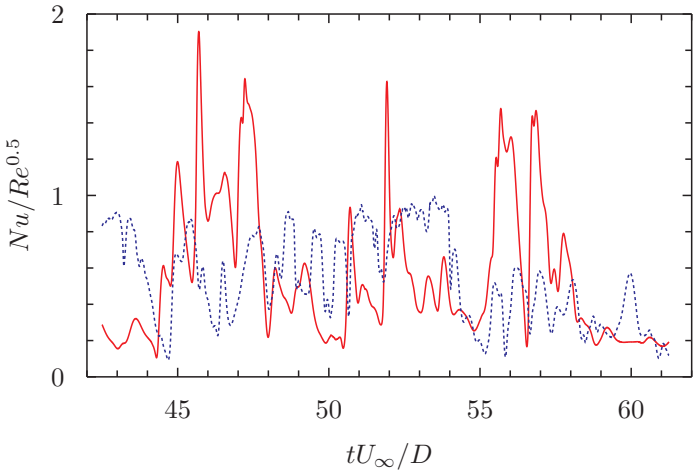

FIGURE 7. Time history of Nusselt number from fine LES (10M cvs) at $Re = 8900$; —— $\phi = 150°$, - - - - $\phi = 180°$.

so a more detailed validation study would require comparison of temperature profiles throughout the cylinder wake.

Acknowledgments

STB was supported under the Dept. of Energy Computational Science Graduate Fellowship (grant number DE-FG02-97ER25308). The authors acknowledge the following NSF award for providing computing resources: MRI-R2: Acquisition of a Hybrid CPU/GPU and Visualization Cluster for Multidisciplinary Studies in Transport Physics with Uncertainty Quantification.

REFERENCES

BOSE, S., MOIN, P. & HAM, F. 2011 Explicitly filtered large eddy simulation on unstructured grids. *Center of Turbulence Research Annual Research Briefs* pp. 87–96.

DENEV, J., FRÖLICH, J., BOCKHORN, H., SCHWERTFIRM, F. & MANHART, M. 2008 DNS and LES of scalar transport in a turbulent plane channel flow at low Reynolds number. *Lecture Notes in Computer Science* **4818**, 251–258.

DONG, S., KARNIADAKIS, G., EKMEKCI, A. & ROCKWELL, D. 2006 A combined direct numerical simulation-particle image velocimetry study of the turbulent near wake. *J. Fluid Mech.* **569**, 185–207.

INAGAKI, M., HATTORI, H. & NAGAONO, Y. 2012 A mixed-timescale SGS model for thermal field at various Prandtl numbers. *International J. of Heat and Fluid Flow* **34**, 47–61.

KHALIGHI, Y., MANI, A., HAM, F. & MOIN, P. 2010 Prediction of sound generated by complex flows at low Mach numbers. *AIAA J.* **48** (2), 306–316.

LEE, J., CHOI, H. & PARK, N. 2010 Dynamic global model for large eddy simulation of transient flow. *Phys. of Fluids* **22**, 075106.

LI, Q., SCHLATTER, P. & HENNINGSON, D. 2011 Comparison of SGS models for passive scalar mixing in turbulent channel flows. *Direct and Large-eddy Simulation VIII* **15**, 131–136.

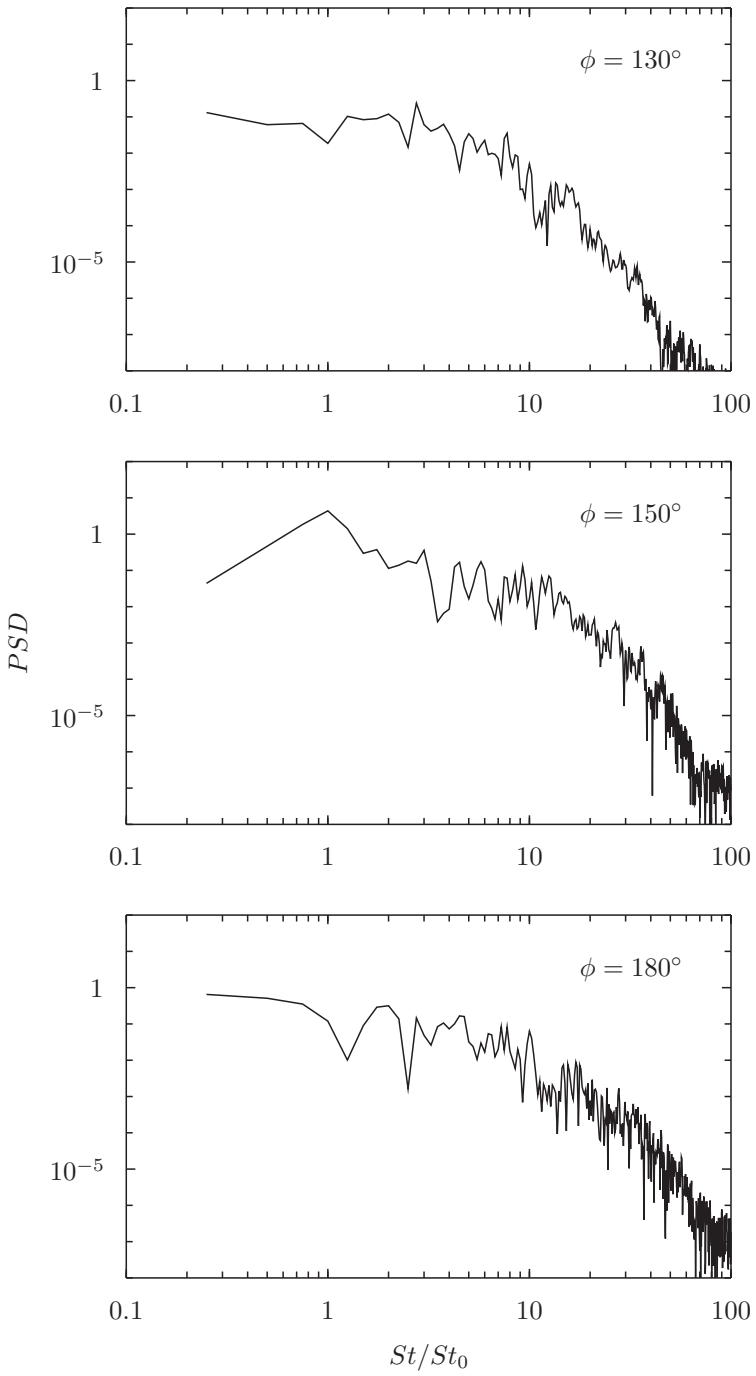

FIGURE 8. PSD of Nusselt number fluctuations from the fine LES (10M cvs) at $Re = 8900$ at three different locations on the rear-side of the cylinder (Welch averaged).

LILLY, D. 1992 A proposed modification of the Germano subgrid-scale closure method. *Phys. of Fluids A* **4**, 633–635.

Moin, P., Squires, K., Cabot, W. & Lee, S. 1991 A dynamic subgrid-scale model for compressible turbulence and scalar transport. *Phys, of Fluids A* **7**, 2736–2757.

Nakamura, H. & Igarashi, T. 2004 Unsteady heat transfer from a circular cylinder for Reynolds numbers from 3000 to 15,000. *International J. of Heat and Fluid Flow* **25**, 741–748.

Schmidt, E. & Wenner, K. 1941 Heat transfer over the circumference of the heated cylinder in transverse flow. *Tech. Rep.* NACA-TM-1050. National Advisory Committee for Aeronautics.

Scholten, J. & Murray, D. 1998 Unsteady heat transfer and velocity of a cylinder in cross flow– I. low freestream turbulence. *International J. of Heat and Mass Transfer* **41** (10), 1139–1148.

Vreman, A. 2004 An eddy-viscosity subgrid-scale model for turbulent shear flow: algebraic theory and applications. *Phys. of Fluids* **16** (10), 3670–3681.

Wang, B.-C., Yee, E., Bergstrom, D. & Iida, O. 2008 New dynamic subgrid-scale heat-flux model for LES of thermal flows based on the general-gradient-diffusivity-hypothesis. *J. Fluid Mech.* **60**, 125–163.

Wang, B.-C., Yin, J., Yee, E. & Bergstrom, D. 2007 A complete and irreducible dynamic SGS heat-flux model based on the strain rate tensor for large-eddy simulation of thermal convection. *International J. of Heat and Fluid Flow* **28**, 1227–1243.

Warhaft, Z. 2000 Passive scalars in turbulent flows. *Ann. Rev. of Fluid Mech.* **32**, 203–240.